Bias-driven spontaneous spin-valley polarization in monolayer transition-metal dichalcogenides

Yuriy G. Semenov and Ki Wook Kim

Phys. Rev. B **93**, 041414 — Published 19 January 2016

DOI: 10.1103/PhysRevB.93.041414

Bias driven spontaneous spin-valley polarization in monolayer transition-metal dichalcogenides

Yuriy G. Semenov[1] and Ki Wook Kim[1,2,*]

[1]*Department of Electrical and Computer Engineering, North Carolina State University, Raleigh, NC 27695, USA*

[2]*Department of Physics, North Carolina State University, Raleigh, NC 27695, USA*

Abstract

A physical mechanism that may enable electrical control of carrier spin-valley polarization is theoretically examined in a monolayer transition-metal dichalcogenide (TMD) structure. The idea is based on the interplay between the strongly spin-orbit coupled nature of the TMD band structure and the exchange interaction with a proximate magnet that can spontaneously lift the valley degeneracy when the carrier density exceeds a certain threshold. The analysis based on the free energy of the system clearly illustrates the desired spin-valley polarization in the TMD layer as well as the accompanied rotational phase transition in the magnetization. Numerical estimates utilizing the WS_2 parameters as an example indicates a sharp transition in the spin-valley polarization over tens of percent at room temperature only with a modest change in the electrochemical potential of a few meV via electrostatic bias. Detection of the predicted phenomenon is expected to be straightforwardly through the corresponding modification in the TMD channel conductance.

PACS numbers: 73.22.Gk, 73.40.-c, 75.70.Ak, 75.70.Cn

Atomically thin two-dimensional (2D) layered materials offer a number of unique opportunities that the quasi-2D structures of conventional bulk crystals cannot access. One such example is the recently proposed concept of valleytronics in the crystals of honeycomb lattice symmetry that often possess two equivalent energy bands at the corners of the Brillouin zone[1]. Similar to other internal degrees of freedom with binary states (e.g., electron spin), valley polarization can lead to a host of novel physical phenomena and provide the basis for practical applications including information processing. In this regard, transition-metal dichalcogenides (TMDs) have become a focus of attention for their finite band gaps as well as the possibility to lift the valley degeneracy via the opposite spin symmetry of the valleys[1,2]. Nonetheless, achieving sufficient valley polarization remains a challenge at room temperature. The obvious approach through an external magnetic field, as it turns out, requires an extreme field strength[3–6]. An alternative attempt based on the optical Stark effect appears to suffer from a similar debacle as it needs a very large electric field (excited by circularly polarized radiation) for a sizable valley splitting[7].

A potential solution to the problem may reside in the phenomenon of the proximity interaction with an adjacent magnet. As in other materials with 2D surface states such as graphene[8–10] or topological insulators[11–13], the spin properties of free carriers in the TMDs can be strongly influenced by the exchange field whose strength may actually exceed the effect of external magnetic fields[14]. It is evident that the proximate magnet would break the time reversal symmetry, leading potentially to the different valley-associated spin splitting and valley polarization even without external magnetic field or optical pumping. Moreover, the valley polarization could be sensitive to the magnetization direction. Indeed, the in-plane magnetization is likely to have no impact on the the energy degeneracy of the valley band structure, while the out-of-plane component is expected to shift the valley extrema in the opposite ways; i.e., enhancing the effect of spin-orbital splitting in one valley and diminishing it in the other. Accordingly, the ability to modulate the magnetization proves to be crucial in the application of the valleytronics concept.

At the first glance, only multiferroic or magneto-electric materials can achieve electrical control of magnetization rotation. However, a careful scrutiny reveals an alternative mechanism that can be triggered self-consistently by spin polarized carriers, i.e., by means of the reciprocal influence of the carrier spin polarization on the magnetization. The spin-valley interlocked band structure of monolayer (ML) TMD is favorable for realizing the in-plane

to the out-of-plane magnetization switching in the form of rotational phase transition as the imbalance in the valley (hence, spin) population can induce the effective exchange field in an adjacent magnetic layer along the latter (i.e., out-of-plane) direction through an interplay.

The purpose of this investigation is to theoretically examine the feasibility of the envisioned physical process under a simple electrical control. The result demonstrates that the strength of the exchange effective field, under a sufficiently large carrier density, can indeed exceed the in-plane magnetic anisotropy field and stabilize the net carrier spin-valley polarizations along with the reoriented magnetization [see the schematic illustrations of Figs. 1(a) vs. 1(b)]. A quantitative description of such spontaneous polarization driven by electrical biases is provided below by using ML WS_2 as an example for the numerical estimates.

The specific structure under consideration, as shown in Fig. 1, consists of a thin dielectric (or insulating) ferromagnet (FM) on top of a sheet of TMD monolayer that is followed by the gate electrode. The in-plane dimensions of the magnet are selected to be sufficiently small to ensure the uniform magnetization $\mathbf{M}$ and yet larger than the carrier mean free path of the TMD layer. The dielectric nature of the magnet permits the use of the given TMD dispersion relation without the concern of significant band modification. The electrochemical potential μ of the system is controlled by the doping as well as the applied gate bias. The entire structure is placed on a substrate for structural integrity. For simplicity, only the TMD region in direct contact with the magnet is considered with no regard to the fringing field.

In the analysis, the governing Hamiltonian accounts for the electrostatic energy including the Coulomb repulsion that counterbalances the accumulation of charges in a small region. This term is usually obtained from the Poisson equation but an accurate calculation requires a host of additional details such as the actual geometry of the structure, the dielectric constant of each material, etc. To avoid the unnecessary complexities, a semi-quantitative treatment is adopted instead, where the Coulomb force inside the small contact region (of size A_0) is approximated by the number of charged particles times a constant C_q that is inverse proportional to $\sqrt{A_0}$. With N carriers and N_0 oppositely charged dopants, the electrostatic energy caused by charging/discharging the area can then be simply expressed as $C_q N(N-N_0)$[15]. A more precise evaluation is not essential for the present investigation.

The corresponding Hamiltonian of the system including the contributions from the ex-

change field $\mathbf{G}$ and the magnetic energy E_m of the magnet becomes

$$H_0 = \sum_{\gamma,\sigma,\sigma',\mathbf{k}} [(\varepsilon_{\gamma,\sigma,\mathbf{k}} - \mu + C_q \Delta N)\delta_{\sigma,\sigma'} + \mathbf{G}(\mathbf{M}) \cdot \mathbf{s}_{\sigma,\sigma'}] a^{\dagger}_{\gamma,\sigma,\mathbf{k}} a_{\gamma,\sigma',\mathbf{k}} + E_m(\mathbf{M}) \,, \tag{1}$$

where $\Delta N = N - N_0$. The index $\gamma = \pm 1$ indicates the K and K' valleys, respectively, with the corresponding momentum vector $\gamma\mathbf{K}$ from the zone center; $\sigma, \sigma' = \pm 1$ denote spin up and spin down along the z axis; and $\mathbf{k}$ is the carrier (electron or hole) wave vector, all for ML TMD. Note that this work adopts the notations either in the electron or the hole picture depending on the sample types (i.e., n-type or p-type, respectively). As such, the carrier energies are generally described by the positive values. Then, the first term in Eq. (1) accounting for the electron/hole energy spectrum in the γ valley of the intrinsic TMD is given as

$$\varepsilon_{\gamma,\sigma,\mathbf{k}} = \frac{\hbar^2(\mathbf{k} - \gamma\mathbf{K})^2}{2m^*} + (1 - \gamma\sigma)\Delta_{\mathrm{SO}} \,, \tag{2}$$

where m^* is the effective mass and $2\Delta_{\mathrm{SO}}$ gives the spin-orbital splitting[16]. While convenient, this is an approximate expression valid only near the conduction/valence band extrema. The second term in the square brackets of Eq. (1) defines the exchange interaction of TMD carriers with the proximate magnet via the effective field $\mathbf{G}(\mathbf{M}) = G\mathbf{m}$, where $\mathbf{m} = \mathbf{M}/|\mathbf{M}|$ and $\mathbf{s}$ represents the Pauli matrices. Then, $a^{\dagger}_{\gamma,\sigma,\mathbf{k}}$ and $a_{\gamma,\sigma,\mathbf{k}}$ are the usual creation and annihilation operators. As such, $\widehat{n} = \sum_{\gamma,\sigma,\mathbf{k}} a^{\dagger}_{\gamma,\sigma,\mathbf{k}} a_{\gamma,\sigma,\mathbf{k}}$ is the operator for the total number of particles with the mean value $\langle\widehat{n}\rangle = N$. The last term in Eq. (1) accounts for the magnetic energy that depends on the intrinsic anisotropy as well as the size and the shape of the magnet. Referring to the detailed analysis of these dependencies in the literature (e.g., Ref. 17), we approximate the magnetic energy by the axial anisotropy term in the form $E_m(\theta) = V_0 K_a \sin^2\theta$, where $V_0 = A_0 d$ is the volume of the magnet (with the thickness d). The anisotropy constant K_a (> 0) establishes the vertical (z) direction as the hard axis and the x-y as the easy plane; θ denotes the angle of $\mathbf{M}$ deviation from the easy plane (toward the hard axis).

Supposing the controllability of μ by the gate bias, the valley polarization and the corresponding magnetization would feed the minimum of the thermodynamic potential $\Omega_c(\theta)$ of the carriers that is partly counteracted by the increase in $E_m(\theta)$. Diagonalization of the spin-dependent part in Eq. (1) redefines the valley extrema and their spin splitting as

$$E^c_{\gamma,\sigma}(\theta) = \Delta_{\mathrm{SO}} - \gamma\sigma\sqrt{G^2 + \Delta^2_{\mathrm{SO}} - 2\gamma\Delta_{\mathrm{SO}} G \sin\theta} \,. \tag{3}$$

It is evident that the in-plane orientation of $\mathbf{M}$ (i.e., $\theta = 0$) retains the energy degeneracy between the conjugated spin states in the K and K' valleys with some lowering of ground energies ($\simeq -G^2/2\Delta_{\rm SO}$ if $G \ll \Delta_{\rm SO}$) due to the mixing with the excited spin states by the exchange field. On the other hand, a canting magnetization lifts the degeneracy such that the previously identical ground state energies of the two valleys [i.e., $(\gamma, \sigma) = (1, 1)$ vs. $(-1, -1)$] are now separated by as much as $2G$ when $\theta = \pm\pi/2$. The resulting asymmetry causes valley repopulation and the corresponding spin polarization that, in turn, can reorient the magnetization through a self-consistent process [see Fig. 1(b)]. The initial trigger (i.e., a slight deviation from the perfectly in-plane magnetization) can come from the ubiquitous thermal fluctuation.

To identify the conditions under which the magnetization rotation leads to a gain in the stability, we need to evaluate the thermodynamic potential of TMD carriers $\Omega_c(\theta) = \sum_{\gamma,\sigma} \Omega_{\gamma,\sigma}(\theta)$ subjected to an exchange field $\mathbf{G}$. The necessary summation (or integration) over the electronic states $\mathbf{k}$ can be expressed in terms of a polylogarithmic function $Li_2(x) = \int_x^0 \ln(1-t)\frac{dt}{t}$ and the reduced electrochemical potential $\mu^* = \mu - C_q \Delta N$,

$$\Omega_{\gamma,\sigma}(\theta) = \frac{k_{\rm B}T}{\zeta} Li_2[-\exp\frac{\mu^* - E^c_{\gamma,\sigma}(\theta)}{k_{\rm B}T}]. \tag{4}$$

The conversion to integration can be justified by the stipulation that the spectrum $\varepsilon_{\gamma,\sigma,\mathbf{k}}$ is dense on the scale of thermal energy $k_{\rm B}T$; i.e.,

$$\zeta = \frac{2\pi\hbar^2}{m^* A_0 k_{\rm B} T} \ll 1. \tag{5}$$

The mean number of free carriers in the corresponding γ,σ states can be found from Eq. (4) as

$$N_{\gamma,\sigma} = \frac{1}{\zeta} \ln\left(1 + \exp\frac{\mu^* - E^c_{\gamma,\sigma}(\theta)}{k_{\rm B}T}\right), \tag{6}$$

and the total mean number in the region A_0 is simply given by $N = \sum_{\gamma,\sigma} N_{\gamma,\sigma}$. Strictly speaking, the band shift induced by the proximity interaction modifies the number of carriers in the area. However, its impact is very minor under typical conditions. For instance, the induced variation is estimated to be less than 1% with the acceptor concentration of over 2×10^{12} cm^{-2} and even a smaller fraction in the corresponding n-type cases, assuming the exchange coupling constant G of 20 meV. Hence, the analysis can proceed with an approximation that both $\Omega_{\gamma,\sigma}(\theta)$ and $N_{\gamma,\sigma}$ are controlled by μ but not affected by the proximate exchange field.

Equation (6) along with Eq. (3) clearly show that the TMD layer acquires spontaneous valley (thus, carrier spin) polarization at a finite θ, i.e., when magnetization deviates from its in-plane direction. This magnetization rotation can be achieved in the manner of orientational phase transition[18,19] that can be controlled, in turn, by μ. Particular values of μ, which realize the spin-valley polarization are defined by the boundaries of neutral state (with $\theta = 0$) instability. Since the angle θ plays the role of order parameter in Landau theory of phase transitions, the boundaries of μ corresponds to the curvature sign change of the total energy $\Omega_c(\theta) + E_m(\theta)$ at $\theta = 0$. An explicit form of the latter condition is

$$\frac{\Delta_{\rm SO}^2}{G^2+\Delta_{\rm SO}^2}\sum_\sigma\left[\frac{e^\xi}{e^\xi+e^{\eta_\sigma}}+\frac{\sigma k_{\rm B}T}{\sqrt{G^2+\Delta_{\rm SO}^2}}\ln(1+e^{\xi-\eta_{-\sigma}})\right]=\Lambda, \tag{7}$$

where $\xi = \mu/k_{\rm B}T$ and $\eta_\sigma = E^c_{1,\sigma}(0)/k_{\rm B}T$. The parameter

$$\Lambda=\frac{2\pi\hbar^2K_ad}{m^*G^2} \tag{8}$$

represents the magnetic stiffness and its reduction due to the exchange interaction with the proximate TMD carriers. Equation (7) can be readily solved with respect to ξ in the limit of large spin-orbital splitting ($\Delta_{\rm SO} \gg G$, $k_{\rm B}T$) that eliminates the effect of excited spin-orbital split states. Under this approximation, which is closely relevant to the valence bands of such TMDs as MoS_2 or WS_2, the spin-valley polarization appears when $\mu > \mu_{\rm cr}$ with

$$\mu_{\rm cr}=-k_{\rm B}T\ln\left(\frac{1}{\Lambda}-1\right). \tag{9}$$

It is not surprising that spontaneous polarization mediated by the out-of-plane rotation of $\mathbf{M}$ favors a small stiffness; that is, $\Lambda < \Lambda_{\rm max}$, where the absolute upper bound for $\Lambda_{\rm max}$ is 1 according to Eq. (9). This condition in turn provides a limit in the strength of the magnetic anisotropy. For instance, the realistic values of $d = 2$ nm, $G = 20$ meV and $m^* = 0.34m_0$ (m_0 being the free electron mass) suggests $K_a < 2.4 \times 10^5$ erg/cm^3 – a criterion that can be satisfied by most known magnetic insulators.

Note that the condition $\mu > \mu_{\rm cr}$ is necessary but not sufficient in the TMD with a finite spin-orbital splitting since thermal population of both spin subbands reduces the effect of the carrier mediated effective field. Increasing the carrier density juxtaposes the Fermi level with the excited spin-orbital subband that reduces spin-valley polarization and can finally return the system to the balanced state with $\theta = 0$. The range of the electrochemical potential

(μ_1, μ_2) that supports the spin-valley polarization can be found from the numerical solutions of Eq. (7) for arbitrary ratios between $\Delta_{\rm SO}$, G, and $k_{\rm B}T$.

For the detailed analysis, a WS_2 based structure is used as a specific example. The corresponding material parameters adopted in the calculations are $\Delta_{\rm SO} = 13.5$ meV and 235 meV for the conduction and the valence bands, respectively, and $m^* = 0.34m_0$, where the small difference between the electron and hole effective masses is ignored[20]. In addition, the values for d and G are set to 2 nm and 20 meV, respectively, as indicated earlier. At a given temperature, this leaves the magnetic anisotropy (thus, the magnetic stiffness Λ) and the electrochemical potential μ as the two main variables in solving Eq. (7). Figure 2 provides the resulting calculation at room temperature (curve 1) for the conduction [(a)] and the valence [(b)] bands. When Λ (thus, K_a) is below a certain maximum $\Lambda_{\rm max}$, two correspondent solutions can be found for μ as indicated by the vertical dashed lines (see, for example, the cases of $\Lambda = 0.01$ and 0.3, respectively). It is the interval between these two μ positions μ_1 and μ_2 (thus, the shaded region), where the imbalance in the free carrier population can be expected between the K and K' valleys. This is a significant departure from the simple picture of Eq. (9), shown by curve 3 in Fig. 2(b), even for the valence band with a sizable $\Delta_{\rm SO}$.

The desired net valley polarization is illustrated by curves 2 as a function of μ in the shaded region. Specifically, this quantity is defined as $P_v(\mu) = (N_\gamma - N_{-\gamma})/(N_\gamma + N_{-\gamma})$ with $N_\gamma = \sum_\sigma N_{\gamma,\sigma}$ while taking $|\theta| = \pi/2$ for $E^c_{\gamma,\sigma}(\theta)$ [Eq. (6)]. The corresponding values for spin polarization can be obtained similarly. The percentage of valley polarization, as shown, reaches the plateau of around 30% ($\sim 60\%$) with a low carrier concentration in the conduction (valence) band, respectively. The condition of low electron or hole densities, in turn, requires a small magnetic anisotropy in the magnet (curve 1). This need for a low magnetic barrier is consistent with the expectation; the magnetization rotation accompanying the stable spin-valley polarization must be fulfilled with only a limited number of available carrier spins. The generally lower values of Λ and μ for the conduction band, in comparison to the counterparts in the valence band, can be understood from $\Delta_{\rm SO}$. The small spin-orbital splitting energy (27 meV vs. 470 meV) makes the population imbalance difficult to realize under a degenerate occupancy.

One key question is: Does the magnetization indeed prefer the 90° rotation to the out-of-plane orientation in the shaded region? To examine this point, it is crucial to trace the

angle $\theta = \theta(\mu)$ that is associated with the minimum of the total energy $\Omega_c(\theta) + E_m(\theta)$, as μ varies over the threshold at μ_1 and μ_2. The calculations exhibit a sharp change of $|\theta(\mu)|$ from 0 (in plane) to $\pi/2$ (out of plane) within an interval of approx. 0.5 meV and back to 0 even more steeply in only 0.1 meV (see the inset to Fig. 3). The seemingly abrupt dependence may be due, in part, to the relative simplicity of the adopted treatment with only the axial anisotropy. When the higher-order terms of the magnetic anisotropy are present[21], the process tends to become more gradual with a prolonged tail end. For instance, an extra account of cubic anisotropy with a magnitude about 10% of the axial term broadens the intermediate range to several meV. However, this contribution is likely rather minor when compared to the practicable range of $\mu_2 - \mu_1$. Thus, the transition between two magnetization configurations can indeed be expected via electrical control in a nearly step-wise manner with a judicious choice of the magnet.

The combination of Figs. 2 and 3 overviews the possible scenarios of spin-valley polarization in a biased FM/TMD structure. At a low "gate" voltage (low μ), the symmetrical valley band structure is preserved with the in-plane magnetization. Such a balanced state remains immutable under any bias conditions provided a strong magnetic anisotropy (i.e., $\Lambda > \Lambda_{\max}$). When the magnetic barrier is sufficiently low, on the other hand, the system can be driven out of the stability, via a appropriate gate bias (with $\mu_1 < \mu < \mu_2$), into an alternative state with the out-of-plane magnetization and spin (and valley) split subbands (hence, polarization). Further increase in the voltage ($\mu > \mu_2$) diminishes the net difference in the carrier population of the different spin subbands and the necessary interplay with the magnetization, leading to the recovery of the easy-plane orientation and the symmetrical band structure. The transitions between the two regimes (i.e., symmetric vs. spin-valley polarized) can occur steeply across the boundary at μ_1 or μ_2, requiring only a small swing in the external voltage.

Another interesting aspect of the spontaneous spin-valley polarization and the accompanied electronic band modification is the impact on the conductance $G(\theta, \mu)$ of the TMD region under the gate. Assuming the relaxation time approximation (i.e., the diffusive regime), the channel conductance can be estimated in terms of the key functional dependencies as

$$G(\theta, \mu) \simeq const \sum_{\gamma,\sigma} \int \tau_{\gamma,\sigma,\mathbf{k}} v_x^2(\gamma, \sigma, \mathbf{k}) \left(-\frac{\partial f}{\partial \varepsilon_{\gamma,\sigma,\mathbf{k}}} \right) d\mathbf{k}, \tag{10}$$

where $\tau_{\gamma,\sigma,\mathbf{k}}$ is the carrier relaxation time, $v_x(\gamma, \sigma, \mathbf{k})$ the group velocity along the channel

direction (e.g., x), and f the Fermi-Dirac distribution function[22]. Subsequently, the magnetoresistive effect can be gauged by simply taking the ratio between the values for the in-plane and out-of-plane magnetization. Strictly speaking, the $\theta = 0$ and $|\theta| = \frac{\pi}{2}$ configurations require disparate electrochemical potentials. However, they can be chosen sufficiently close to each other (i.e., only a few meV apart by taking advantage of the very steep transition discussed above) such that the difference can be ignored for the purpose of the conductance calculation at room temperature. Then, the desired magnetoresistance can be approximated as $[G(\theta = 0, \mu)/G(|\theta| = \frac{\pi}{2}, \mu)] - 1$, where μ follows the rotational phase transition boundary defined by curve 1 in Fig. 2.

For numerical evaluation, details on the carrier scattering processes are required. In the present analysis, we focus on the intrinsic, unavoidable interaction with the lattice. More specifically, the energy dependent carrier-phonon scattering rates are taken from the first principles calculations[20], which are then approximated by a series of step functions in each spin-valley subband. The obtained magnetoresistance is plotted in Fig. 4. The result clearly illustrates that the spontaneous spin-valley polarization can lead to modulation of the channel resistance by as much as approx. 40 % in the p-type samples (i.e., the valence band; solid curve) via a small change in the applied electrostatic bias. The effect is the most prominent when the transition occurs with the electrochemical potential near the valence band edge. The correspondent outcome in the n-type cases (i.e., the conduction band; dashed curve) is substantially weaker due to the small spin-obit spitting while, at a few percent, it is still experimentally detectable.

In summary, we propose and theoretically demonstrate the possibility of spontaneous spin-valley polarization in a strongly spin-orbit coupled TMD monolayer that is mediated by the orientation phase transition in an adjacent magnet. The analysis illustrates that a large spin-orbital splitting and a strong proximity exchange interaction are the key conditions necessary to overcome the magnetic anisotropy of a hard magnet. The consequential valley (as well as spin) separating phase transition can be driven electrically through a rather modest change in the carrier densities, which can then be detected rather straightforwardly through the accompanied modification in the TMD channel conductance. The predicted non-linear response to an electrical bias can have a major implication in the prospective valleytronic applications in novel logic and memory[23,24]. The polarization effect may become even more pronounced in the magnetically doped TMDs.

This work was supported, in part, by FAME (one of six centers of STARnet, a SRC program sponsored by MARCO and DARPA).

* kwk@ncsu.edu

[1] See, for a recent review, X. Xu, W. Yao, D. Xiao, and T. F. Heinz, Nat. Phys. **10**, 343 (2014).

[2] S. Z. Butler, S. M. Hollen, L. Cao, Y. Cui, J. A. Gupta, H. R. Gutiérrez, T. F. Heinz, S. S. Hong, J. Huang, A. F. Ismach, E. Johnston-Halperin, M. Kuno, V. V. Plashnitsa, R. D. Robinson, R. S. Ruoff, S. Salahuddin, J. Shan, L. Shi, M. G. Spencer, M. Terrones, W. Windl, and J. E. Goldberger, ACS Nano **7**, 2898 (2013).

[3] Y. Li, J. Ludwig, T. Low, A. Chernikov, X. Cui, G. Arefe, Y. D. Kim, A. M. van der Zande, A. Rigosi, H. M. Hill, S. H. Kim, J. Hone, Z. Li, D. Smirnov, and T. F. Heinz, Phys. Rev. Lett. **113**, 266804 (2014).

[4] D. MacNeill, C. Heikes, K. F. Mak, Z. Anderson, A. Kormányos, V. Zólyomi, J. Park, and D. C. Ralph, Phys. Rev. Lett. **114**, 037401 (2015).

[5] A. Srivastava, M. Sidler, A. V. Allain, D. S. Lembke, A. Kis, and A. Imamoglu, Nat. Phys. **11**, 141 (2015).

[6] G. Aivazian, Z. Gong, A. M. Jones, R.-L. Chu, J. Yan, D. G. Mandrus, C. Zhang, D. Cobden, W. Yao, and X. Xu, Nat. Phys. **11**, 148 (2015).

[7] E. J. Sie, J. W. McIver, Y.-H. Lee, L. Fu, J. Kong, and N. Gedik, Nat. Mater. **14**, 290 (2015).

[8] Y. G. Semenov, K. W. Kim, and J. M. Zavada, Appl. Phys. Lett. **91,** 153105 (2007).

[9] H. X. Yang, A. Hallal, D. Terrade, X.Waintal, S. Roche, and M. Chshiev, Phys. Rev. Lett. **110**, 046603 (2013)

[10] P. Lazić, G. M. Sipahi, R. K. Kawakami, and I. Žutić, Phys. Rev. B **90**, 085429 (2014).

[11] M. Z. Hasan and C. L. Kane, Rev. Mod. Phys. **82**, 3045 (2010).

[12] B. D. Kong, Y. G. Semenov, C. M. Krowne, and K. W. Kim, Appl. Phys. Lett. **98**, 243112 (2011).

[13] H. Ji, J. M. Allred, N. Ni, J. Tao, M. Neupane, A. Wray, S. Xu, M. Z. Hasan, and R. J. Cava, Phys. Rev. B **85**, 165313 (2012).

[14] J. Qi, X. Li, Q. Niu, and J. Feng, Phys. Rev. B **92**, 121403(R) (2015).

[15] This estimate is based on the Hartree approximation of the electronic energy. See, for instance, C. Kittle, *Quantum Theory of Solids* (Wliey, New York, 1963), Chap. 5.

[16] H. Rostami, A. G. Moghaddam, and R. Asgari, Phys. Rev. B **88**, 085440 (2013).

[17] Y. G. Semenov, X. Duan, and K. W. Kim, Phys. Rev. B **86**, 161406(R) (2012).

[18] H. Horner and C. M. Varma, Phys. Rev. Lett. **20**, 845 (1968).

[19] J. J. Alonso and J. F. Fernandez, Phys. Rev. B **74**, 184416 (2006).

[20] Z. Jin, X. Li, J. T. Mullen, and K. W. Kim, Phys. Rev. B **90**, 045422 (2014).

[21] L. D. Landau and E. M. Lifshitz, *Electrodynamics of Continuous Media* (Pergamon, New York, 1984), Chap. 5.

[22] P. Y. Yu and M. Cardona, *Fundamentals of Semiconductors*, (Springer, New York, 2002), Chap. 5.

[23] K. Galatsis, K. Wang, Y. Botros, Y. Yang, Y.-H. Xie, J. F. Stoddart, R. B. Kaner, C. Ozkan, J. Liu, M. Ozkan, C. Zhou, and K. W. Kim, IEEE Circuits Devices Mag. **22**, 12 (2006).

[24] K. Galatsis, A. Khitun, R. Ostroumov, K. L. Wang, W. R. Dichtel, E. Plummer, J. F. Stoddart, J. L. Zink, J. Y. Lee, Y.-H. Xie, and K. W. Kim, IEEE Trans. Nanotechnol. **8**, 66 (2009).

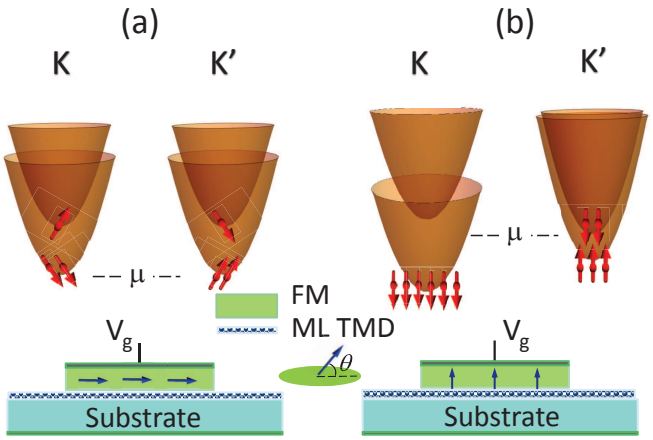

FIG. 1. (Color online) Schematic illustration of the TMD-FM structure for the electrically controlled spin-valley polarization accompanied by the magnetization rotation. (a) At low carrier densities, both K and K' valleys are symmetrically occupied (thus, no net spin polarization in the out-of-plane z direction) and the FM magnetization is along the easy plane. (b) When the carrier density increases, the spontaneous spin polarization induced by the interplay with the magnet may eventually exceed the magnetic anisotropy field and stabilize the net carrier spin-valley polarization along with the magnetization reoriented in the z direction. The K and K' bands are plotted from the perspective of electrons (or holes) for the n-type (or p-type) cases, respectively.

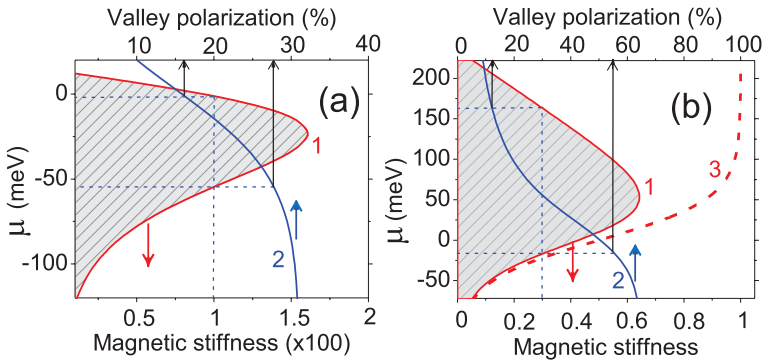

FIG. 2. (Color online) Critical values of electrochemical potential (curve 1) as a function of the magnetic stiffness Λ calculated for (a) n-type and (b) p-type ML WS_2 at room temperature [Eq. (8)]. The shaded region denotes the conditions under which the spin-valley polarization and the reoriented magnetization can be observed. Thus, curve 1 can be viewed as the boundary that separates two different "phases". Curve 3 in (b) shows the ideal case scenario when the spin-orbital splitting is very large. The reference of μ (i.e., zero) is set to the bottom of the conduction band [(a)] and to the top of the valence band [(b)], respectively. A negative value of μ indicates the electrochemical potential in the energy gap between the conduction and valence bands in both cases. Curves 2 shows the percentage of valley polarization in the shaded region at the corresponding electrochemical potential. The dashed lines are provided to aid interpretation of the results. With the magnetic stiffness of 0.01 in (a), for instance, the upper and lower bounds for the shaded region can be found in terms of μ (curve 1), which then illustrate the respective valley polarization of 27% and 12% (curve 2; see thin black arrows). An example of $\Lambda = 0.3$ is given likewise in (b). Note that, while similarly polarized, the percentages of net carrier spin take different numerical values.

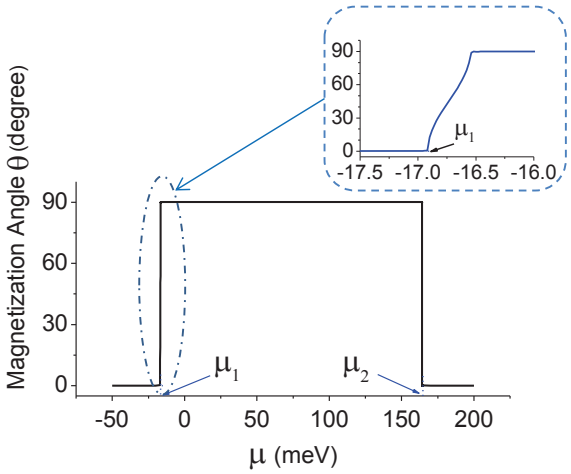

FIG. 3. (Color online) Magnetization orientation as a function of μ illustrating the rotational phase transition between the in-plane ($\theta = 0$) and out-of-plane ($|\theta| = \frac{\pi}{2}$) states. The parameters used in the calculation are identical to those of Fig. 2(b) with $\Lambda = 0.3$ (i.e., the valence band in a p-type sample). The inset provides a more detailed picture of the transition around μ_1.

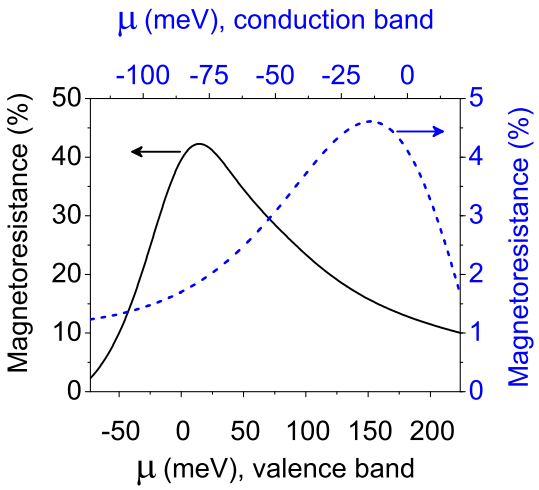

FIG. 4. (Color online) Magnetoresistance of n-type (blue, dashed) and p-type (black, solid) ML WS_2 mediated by the rotational phase transition in the magnetization (from the in-plane to the out-of-plane state). For each value of μ, it is assumed that the system meets the conditions specified by curve 1 in Fig. 2(b). The reference point ($\mu = 0$) is at the bottom of the conduction band (n-type) and at the top of the valence band (p-type), respectively, as described before.